A study of seasonal rainfall in Vietnam at the end of 21st century according to the Non-Hydrostatic Regional Climate Model

Mau Nguyen-Dang[1*], Truong Nguyen-Minh[2], Hidetaka SASAKI[3], Izuru TAKAYABU[3]

[1]*Vietnam Institute of Meteorology, Hydrology and Climate change*
[2]*Hanoi University of Science, Hanoi, Vietnam,*
[3]*Meteorological Research Institute, Tsukuba, Japan*

Received 6 May 2018; accepted 13 August 2018

Abstract:

This article presents analyses of changes in the seasonal characteristics of the far future climate (2080-2099) across Vietnam as projected by the Non-Hydrostatic Regional Climate Model (NHRCM) in terms of the RCP 8.5 (Representative Concentration Pathways 8.5) scenario. The results show significant changes in seasonal rainfall in Vietnam compared with the 1982-2003 baseline period. Specifically, the June-August rainfall is projected to increase in South Central (SCVN), Central Highlands (CHVN), and South Vietnam (SVN), but to decrease by approximately 50% in North Central (NCVN) and off the Central coast. In the September-November season, the NHRCM detects an increase in rainfall of about 50% in North Vietnam (NVN) and CHVN. The increase and decrease in rainfall are due to the convergence and divergence of moisture flux that might be associated with the westward expansion of the Northwestern Pacific High Pressure in the far future.

Keywords: **geopotential height, moisture flux, NHRCM model, rainfall, 850 hPa winds.**

Classification number: **6.2**

Introduction

Rainy season in Vietnam

During the Asian summer monsoon, the main winds in the lower atmospheric layers (from the above ground to 500 hPa) are from the south-west, and from the north-east in the higher atmospheric layers (above the 500 hPa atmospheric layer) [1]. The summer monsoon circulation shifts north-eastwards from the southern hemisphere (north of Australia), crossing the equation in the Indian Ocean, to Vietnam. The positive activity of the summer monsoon circulation brings substantial moisture from the warm Indian Ocean to generate the rainy season across Vietnam. However, much of the variability of the summer monsoon and its weather events are due to the reasons listed below.

1) Variability of large-scale circulations

Figure 1 shows the Asian-Pacific summer monsoon regions. The Asia-Pacific region is divided into three summer monsoon systems: India, East Asia, and the Pacific Northwest [2]. According to Fig. 1, Vietnam is located in the interaction region of the Asia-Pacific summer monsoon systems. As a result, the variability of the summer monsoon and its weather events across Vietnam clearly depends on the variability of these Asian-Pacific summer monsoon regions.

During the summer months, the wind and airstream flowing near the ground are south-west to south and south or south-east to north. The air flow prevailing in Vietnam is equatorial and tropical, originating in the southern hemisphere and the tropical sea as well as the North Pacific high pressure [1]. In addition, during the pre-onset and summer, westerly winds originating in the South Asian low pressure [1] and the extratropical region [3] also effect NVN.

*Corresponding author: Email: mau.imhen@gmail.com

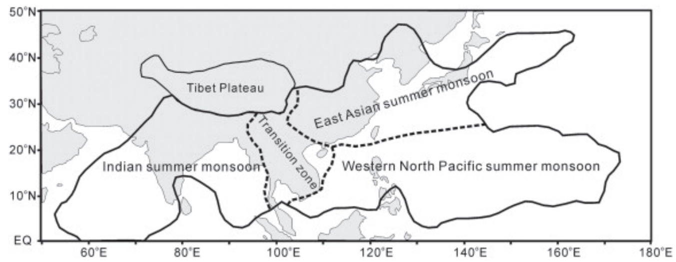

Fig. 1. The three summer monsoon regions of the Asian-Pacific summer monsoon: Indian summer monsoon (ISM), East Asian summer monsoon (EASM), West North Pacific summer monsoon (NWPSM) [2].

2) Variability of El Niño Southern Oscillation (ENSO)

The ENSO is the major factor causing variability in the summer monsoon in Vietnam [1-3]. In Vietnam, the onset date of summer monsoon and its rainy season is later in the El Niño phase and earlier in the La Niña phase [4, 5]. In most of the climatic regions of Vietnam, the total rainfall in the summer monsoon is below normal in the El Niño phase and above normal in the La Niña phase.

3) Local-scale factors

Figure 2 shows that Vietnam is a part of Southeast Asia and is bordered by the Western Pacific to the east, China to the north, and Cambodia and Laos to the west. Topography plays an important role in variability of the monsoon [1]. During the summer monsoon, the mountains in Western Vietnam, especially Truong Son, and in Laos cause a Foehn effect, changing the humid and hot characteristics of the wind from the Bay of Bengal and causing the very hot and dry weather event in the Central region (CVN). A Foehn wind is also referred to as a hot-dry west wind, or Laos wind, that often occurs in NVN and the CVN.

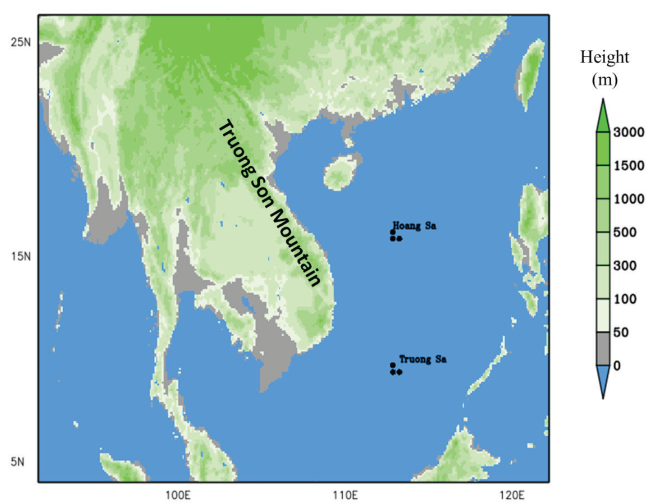

Fig. 2. The terrain map of Vietnam derived from terrain of NHRCM model.

Due to topography, a depression, the 'Bac Bo depression', is formed above the northern Indochinese Peninsula. It primarily causes hot weather over mountainous areas in NVN and Laos. This depression is a region of wind convergence. It causes the wind to change direction from south-west to south-east, blowing over the Gulf of Tonkin and heading towards the north of Vietnam (it often occurs in the northeast and Red River Delta). Due to characteristics of geography, territory, and topography, monsoon circulation in Vietnam is typical, complex, and difficult to forecast.

4) The rainy season and the mesoscale factor

As result of the abovementioned factors, the climate in Vietnam varies significantly, especially the rainfall during the rainy season. In general, the climate in Vietnam is divided into rainy and dry seasons.

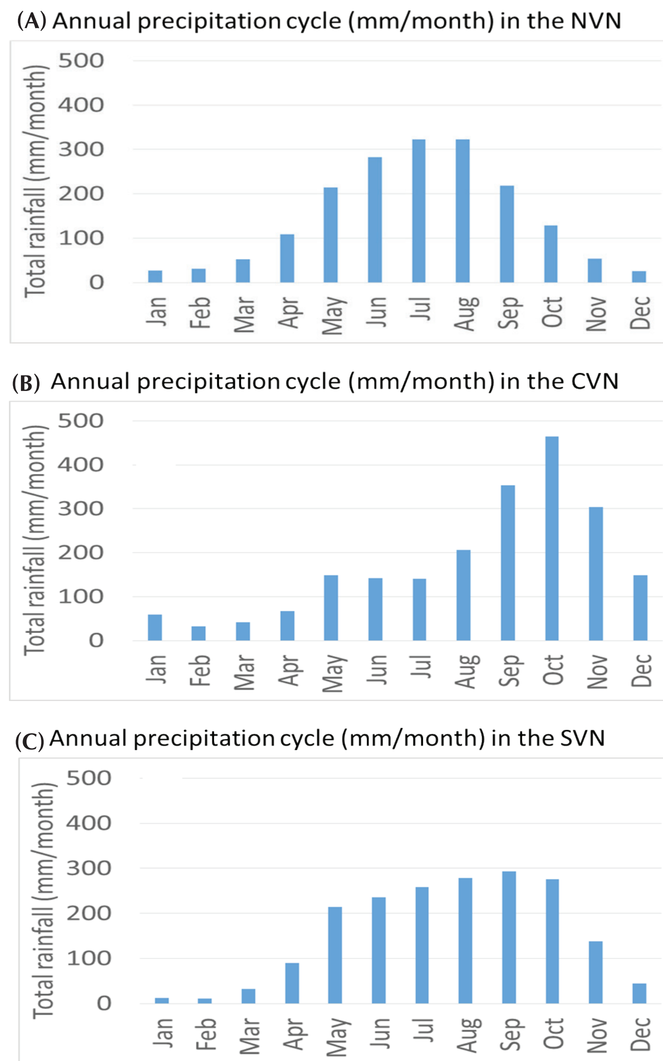

Fig. 3. Annual precipitation cycle in NVN (A), CVN (B), and SVN (C) calculated from observed data from 150 stations, 1961-2014.

Figure 3 shows that the rainy season is from May to November in NVN, CHVN, and SVN; and from September to December in CVN. The rainy season is driven by the summer monsoon in NVN, CHVN, and SVN. However, the rainy season in NCVM and SCVN is driven by cold fronts and tropical cyclones (TCs) [1]. The peak duration of the rainy season is similar to the peak duration of TCs in the East Vietnam Sea, with the two to three TCs per month. The peak duration of the rainy season in CVN is close to the high frequency of TCs and cold fronts.

Projection of seasonal rainfall

The global climate system is expected to undergo significant changes in the future in terms of the greenhouse gas (GHG) scenarios. By the end of the 21st century, the global average temperature will increase by 4°C compared to the baseline scenario of RCP 8.5 [6]. RCP8.5 is a so-called 'baseline' scenario that does not include any specific climate mitigation target. The greenhouse gas emissions and concentrations in this scenario increase considerably over time, leading to a radiative forcing of 8.5 W/m^2 at the end of the century. Projections show that the summer monsoon is expected to be stronger. These projections also show the earlier onset and latter withdrawal date, which will lead to a longer rainy season [6]. In recent years, many studies have mentioned the impact of the increase of GHG concentration on summer monsoon variability. However, very high uncertainty projections in terms of scenarios for summer monsoon variability are found in the studies. According to projections, the general trend is that summer monsoon rainfall is expected to increase with global warming [6-8]. The extreme rainfall events caused by heavy rains are expected to increase in the ISM region [9].

In Vietnam, climate projection studies have been considered in some research [10-12]. The projections for changes in the summer monsoon and its rainfall have been considered by using the PRECIS (Providing REgional Climates for Impacts Studies) [13] and CCAM (Conformal Cubic Atmospheric Model) models [12].

In this study, we focus on the assessment of the rainy season and the amount of rain. In particular, changes in seasonal rainfall in Vietnam by the end of 21st century are investigated using the NHRCM to simulate climate in the baseline period (1982-2003) and to project the far future climate (2080-2099) in terms of the RCP 8.5 scenario. In the next section, data and model configuration are presented. The results and conclusion are presented in the below section.

Data and analysis

The 850 hPa winds from CFSR (Climate Forecast System Reanalysis) of the NCEP (National Centers for Environmental Prediction) [14] are used to validate 850 hPa wind simulations.

The daily gridded precipitation of the Asian Precipitation Highly-Resolved Observational Data Integration towards Evaluation (Aphrodite) [15] is used to validate distributions of simulated rainfall over the entire domain.

The NHRCM used in this study is the extended version of the Non-Hydrostatic Model (NHM), in which the soil model is replaced by MRI (Meteorological Research Institute)-Simple Biosphere model [16], and lateral boundary conditions are replaced by spectral nudging boundary conditions. A detailed description of the NHRCM can be found in K. Saito, et al. (2006) [17]. The model is able to simulate the regional climate and dynamically downscale from Atmospheric General Circulation Model (AGCM) outputs for the Japan [18, 19] and Vietnam [20] regions.

The model domain covers a region of about 85°E -130°E and 5°S-35°N, with a 10 km horizontal grid spacing and 40 vertical levels. The initial and boundary conditions for the NHRCM are the MRI-AGCM3.2 outputs with a 20 km horizontal grid spacing, supplied by the SOUSEI Programme.

Results and discussion

In this section, we examine seasonal characteristics and compare the changes predicted by the 2080-2099 projections with the 1982-2003 simulations, focusing on main rainy months of June-August (JJA) and September-November (SON).

850 hPa Winds Simulations

The JJA 850 hPa wind averages for the period 1982-2003 are shown in Figure 4A for CFSR, and in Figure 6A for NHRCM's simulation. The Figure 4A shows the development of the south-west winds in the 850 hPa layer during summer monsoon season. The significant feature is that the south-west wind will cover most of the Indochina Peninsula and then extend over the eastern Philippines. The monsoon trough occurs due to the development of the south-west winds and its axis crosses NVN in the north-west-south-east direction.

A comparison of Fig. 6A with Fig. 4A shows that the development of the south-west winds and monsoon trough are well simulated by the NHRCM model. However, the monsoon trough in the simulation and intensity of the south-west winds (Fig. 6A) are stronger than in the CFSR (Fig. 4A). In addition, the meridional winds simulated (Fig. 6A) are weaker in intensity in the northern East Vietnam sea than they are in the CFSR (Fig. 4A).

Figure 4B shows the SON 850 hPa wind averages for the period1982-2003 from CFSR data and the corresponding NHRCM winds (Fig. 7A). In Figure 4B, the east winds are in the northern area and the west winds in the southern area. The comparison shows that the NHRCM model simulates stronger east winds (Fig. 7A) than does CFSR (Fig. 4A). However, the model shows weaker west winds (Fig. 8A) in the southern area than does the CFSR (Fig. 4B).

These comparisons show that the NHRCM model well captures the JJA and SON circulations. However, the wind speed and monsoon trough during the JJA season is stronger than in CFSR. In addition, the wind speed during SON season is weaker than in CFSR.

Rainfall simulations

Figure 5 shows the mean of JJA and SON rainfall averaged during 1982-2003 calculated from the Aphrodite data and the corresponding NHRCM rainfall is shown in the Fig. 6A and Fig. 7A, respectively.

The comparison of Fig. 5A with Fig. 6A indicates that the spatial distribution of JJA rainfall simulation is quite similar to that of Aphrodite. However, there is a quite clear difference in the JJA rainfall, which is higher in the simulation than in Aphrodite. The clearest error in simulation of JJA rainfall can be found in the area to the west of the Truong Son mountains. In addition, an underestimation in rainfall simulation can be found in southern CVN. These results show that the NHRCM model overestimates the rainfall due to summer monsoon, and underestimates rainfall due to Foehn wind effects.

Results in Fig. 5B and Fig. 8A show that the spatial distribution of SON rainfall in the NHRCM model is similar to that of Aphrodite. However, the rainfall simulation is higher than that of Aphrodite, especially in NCVN.

Generally, the JJA and SON simulations have the same spatial distribution as that of Aphrodite. However, the model tends to capture the higher rainfall due to JJA and SON monsoon circulations. Additionally, the lower rainfall due to Foehn wind effects on the eastern side of the Truong Son mountains during JJA season is simulated.

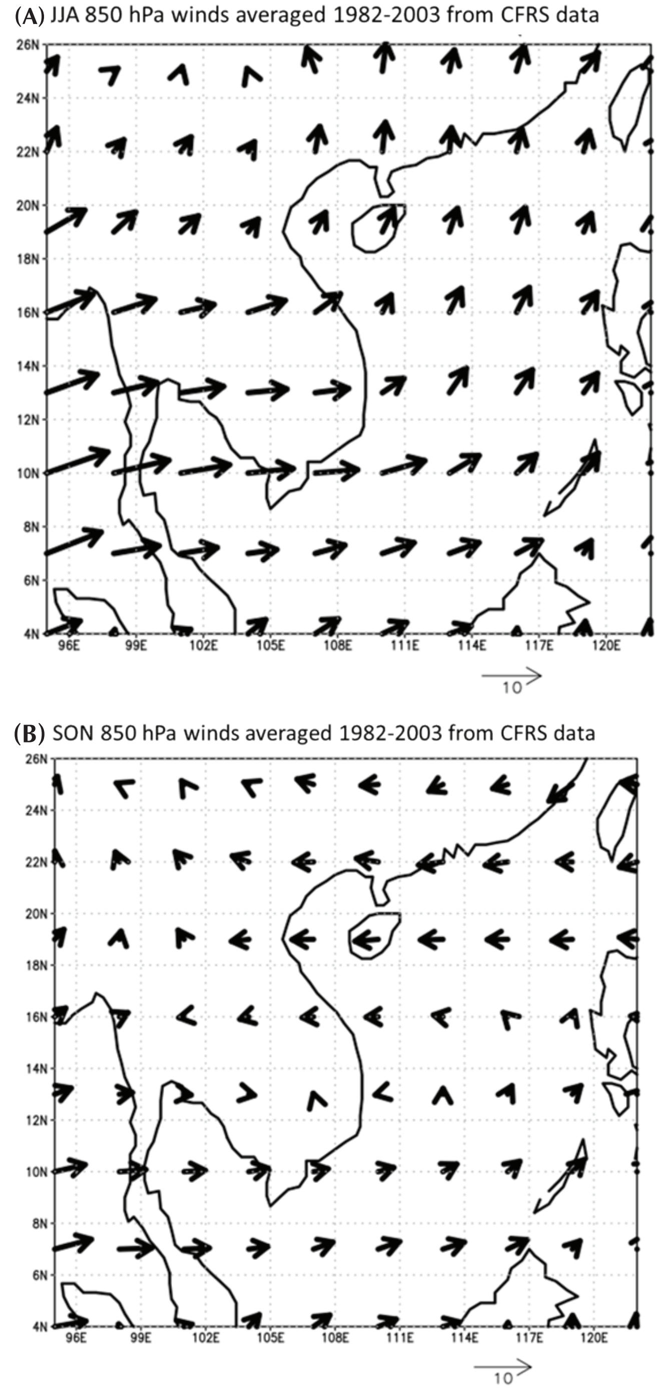

Fig. 4. CFSR mean 850 hPa winds, 1982-2003 (m/s): (A) JJA and (B) SON.

Seasonal rainfall projection for the end of 21st century (far future)

Figure 6 shows the 850 hPa winds and daily rainfall in JJA at present and in the far future climate, simulated and projected by the NHRCM model. It can clearly be seen that the south-westerly summer monsoon prevails in Southeast Asia and the East Sea of Vietnam. Heavy rainfall belts

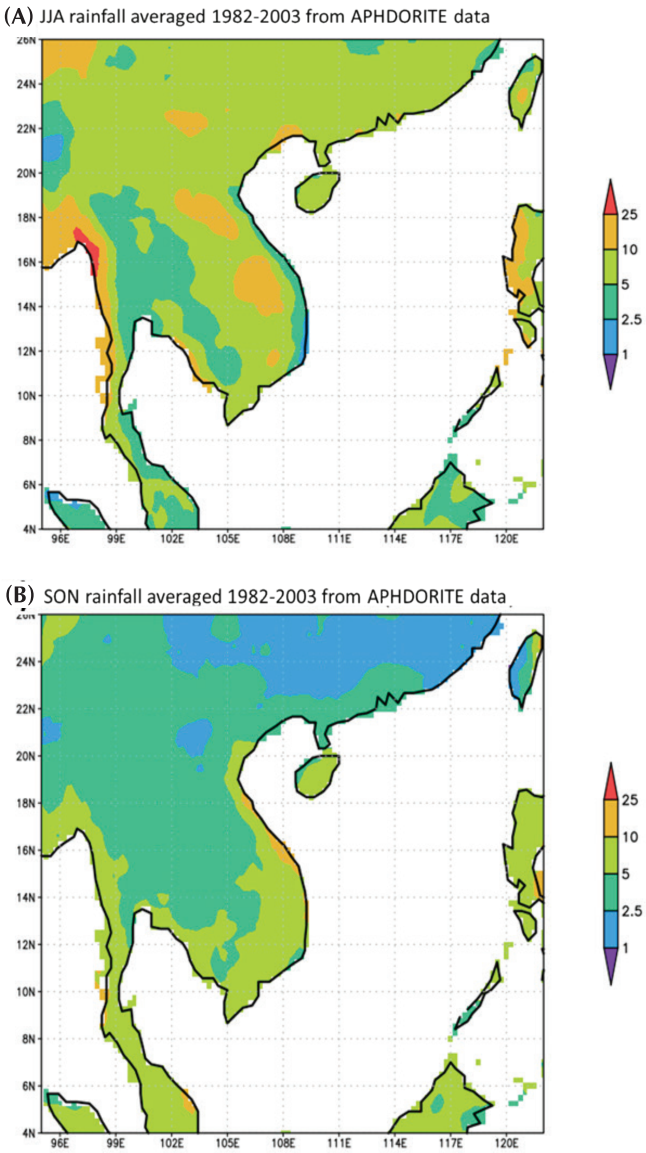

Fig. 5. (A) JJA rainfall (mm/day) and (B) SON rainfall (mm/day), 1982-2003, from Aphrodite.

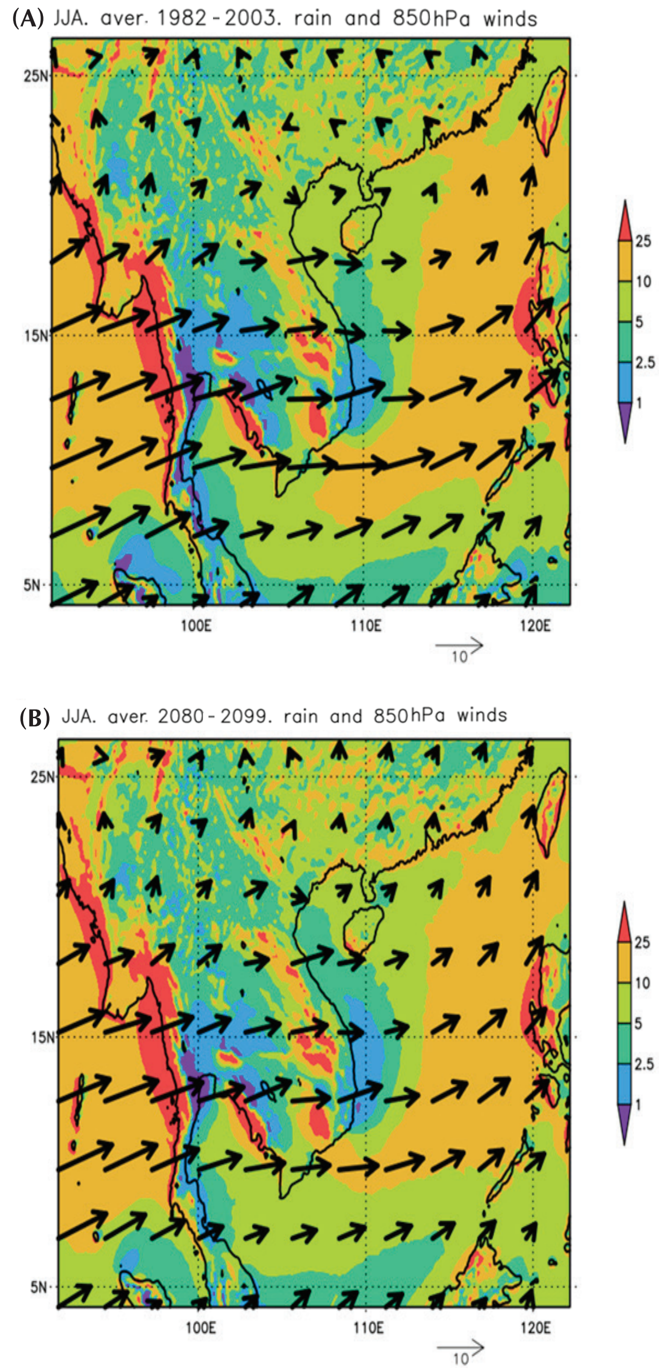

Fig. 6. JJA rainfall (mm/day) and 850 hPa winds (m/s) from NHRCM for (A) 1982-2003 and (B) 2080-2099.

are found along the western coast of Thailand, Cambodia, and along the border between Laos and Vietnam, where a mountain range located (also refer to Kieu-Thi, et al., 2016). There is a small area of the South-Central coastal region where upwelling with low sea-surface temperature is often observed.

The SON pattern is presented in Fig. 7. A heavy rainfall belt is located on the windward side of the mountain range that blocks easterly winds to the North of 15°N (i.e., the trade winds) from the tropical Western Pacific. A cyclonic circulation dominates over the East Sea of Vietnam that seems to weaken in far future (Fig. 7B).

Distributions of changes in 850 hPa winds and rainfall in JJA and SON between far future and the baseline period are shown in Fig. 8. During JJA season in 2080-2099, rainfall should increase by about 40% compared to the baseline rainfall in SCVN, CHVN, and SVN. However, a considerable decrease in rainfall can be found in NCVN.

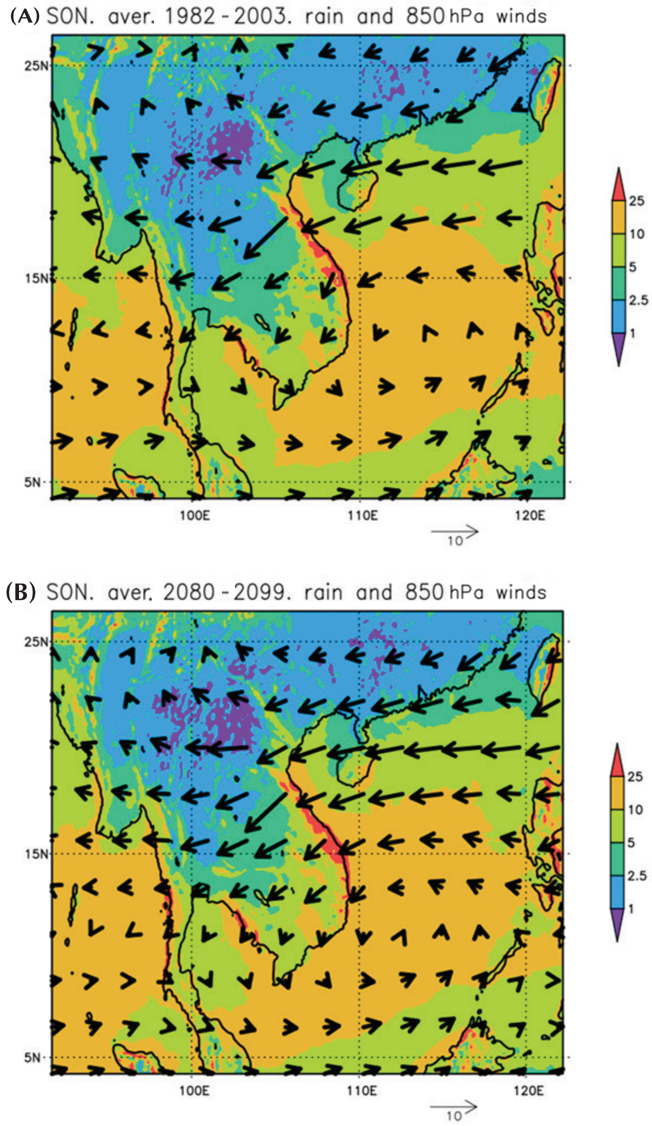

Fig. 7. Same as Fig. 6 but for SON values.

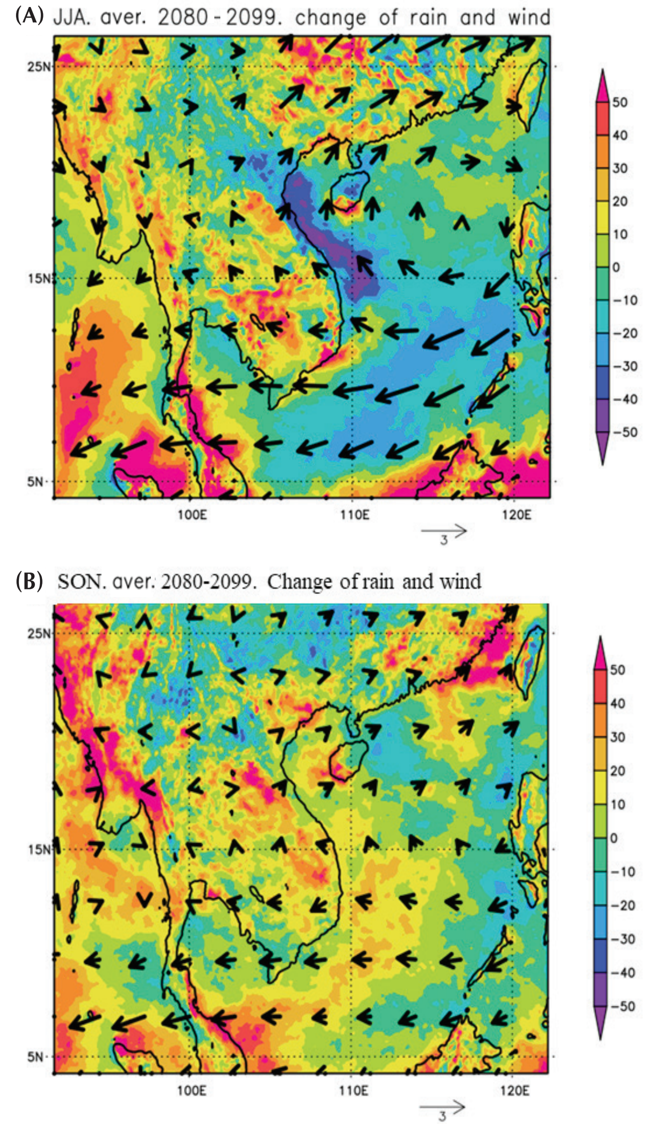

Fig. 8. Changes in 850 hPa winds and total rainfall (%) in JJA (A) and SON (B) for the 1982-2003 and 2080-2099 periods.

850 hPa wind anomalies describe an anticyclonic circulation over the East Sea of Vietnam that is expected to modify moisture flow toward sub-regions of Vietnam in the summer months (Fig. 8A).

During SON season, the NHRCM model shows an increase in 2080-2099 rainfall over most of the country compared to the baseline. The most noticeable increase is of approximately 50% in NVN and CHVN (Fig. 8B). An anticyclonic circulation anomaly is also found over the East Sea of Vietnam; however, it is much weaker than that in JJA.

To explore the reasons for the changes in 850 hPa winds and rainfall mentioned above, we calculated the changes in 850 hPa geopotential height (GHT) and 850-500 hPa vertically integrated moisture flux (IMF) in the far future compared to the baseline period. In general, GHT increases in the entire domain in the far-future climate (Fig. 9). However, Fig. 9A indicates a strong positive anomaly over the East Sea of Vietnam in JJA that helps explain the anticyclonic anomaly mentioned above. IMF is expected to diverge off the CVN coast but converge in SCVN, CHVN, and SVN (Fig. 9), where rainfall increases and decreases, respectively.

Similar to the JJA case, a positive GHT anomaly is also observed over the East Sea of Vietnam in SON, but it is weaker than that in JJA. This means that the Northwestern Pacific Subtropical High (NPH) will be stronger over this sea area in the far future. Due to the westward expansion of NPH toward the East Vietnam Sea, IMF is expected to increase in inland Vietnam. Convergence of IMF will probably to occur in NVN and CHVN where rainfall increases. The strongest IMF is found to the south of 15°N from the tropical Western Pacific towards the Bay of Bengal.

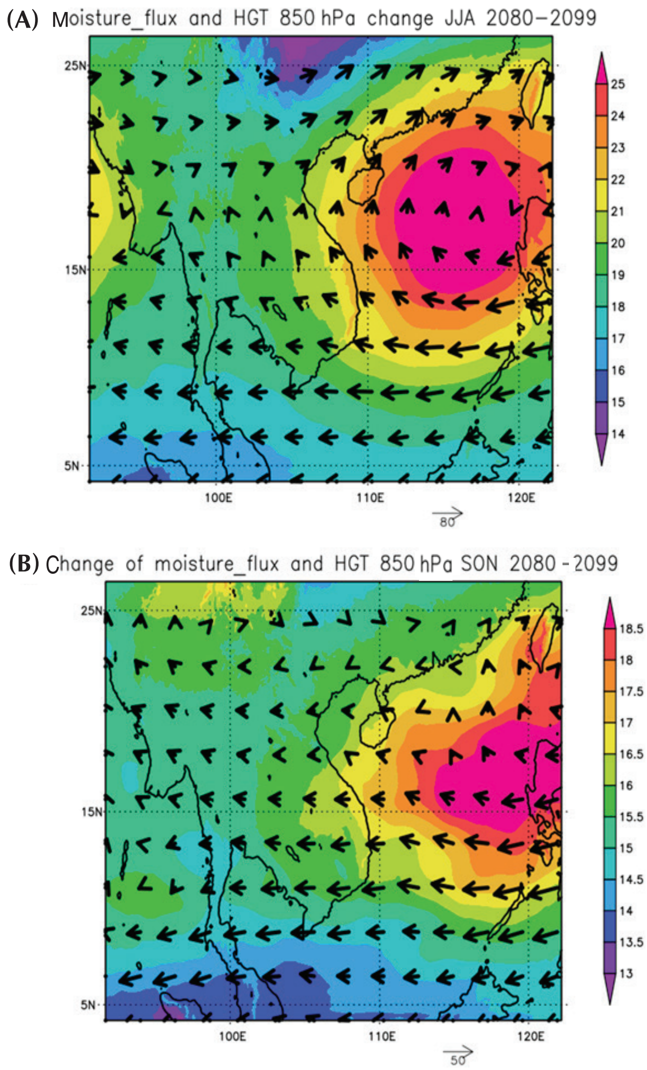

Fig. 9. Same as Fig. 8 but for 850 hPa GHT (m) and 850-500 hPa IMF (kg/kg/m/s).

Conclusions

Using the RCP8.5 emission scenario, the NHRCM model indicates clear changes in seasonal characteristics over the Vietnam region by the end of the 21st century compared to the present climate. Rainfall and 850 hPa wind patterns in the 2080-2099 period are similar to those of the 1982-2003 period, illustrating the influences of the south-westerly summer monsoon and NPH. Rainfall is projected to increase to about 40% in SCVN, CHVN, and SVN; however, it decreases to 50% in NCVN and off the CVN coast due to the projected IMF divergence. Conversely, the rainfall increase may be owing to stronger moisture flux convergence. For the SON season, rainfall is projected to increase to 50% in NVN and CHVN compared to the present climate. This increase in rainfall can be explained by the stronger NPH that will bring more moisture towards inland Vietnam in the far future.

ACKNOWLEDGEMENTS

This work was conducted with the co-operation of Development of Basic Technology for Risk Information on Climate Change, supported by the SOUSEI Programme of the Ministry of Education, Culture, Sports, Science, and Technology of Japan. The authors thank the Ministry of Land, Infrastructure, Transport, and Tourism for funding travel expenses between Vietnam and Japan.

REFERENCES

[1] N.D. Ngu and N.T. Hieu (2004), *Climate and Climate Resources in Vietnam,* Agricultural publisher, Hanoi.

[2] B. Wang, LinHo (2002), "Rainy season of the Asian-Pacific summer monsoon", *Journal of Climate,* **15**, pp.386-398.

[3] B. Wang, LinHo, Zhang, Yongsheng, M.-M. Lu (2004), "Definition of South China Sea monsoon onset and commencement of the East Asia summer monsoon", *Journal of Climate,* **17(4)**, pp.699-710, DOI:10.1175/2932.1.

[4] N.D. Ngu, et al. (2003), *Impact of ENSO on weather, climate, environment and socio-economic in Vietnam*, Final report of the national project.

[5] N.T.H. Thuan (2008), *Impact of ENSO on summer monsoon and rainfall in the South Vietnam*, PhD thesis, Vietnam Institute of Meteorology, Hydrology and Climate change.

[6] IPCC (2013), *IPCC fifth assessment report: climate change 2013 - The physical science basis*, Cambridge University Press, Cambridge, UK, 1535pp.

[7] R.H. Kripalani, A. Kulkarni, S.S. Sabade (2003), "Indian monsoon variability in a global warming scenario", *Nat. Hazards,* **29**, pp.189-206.

[8] P.C. Hsu, T. Li, J.J. Luo, H. Murakami, A. Kitoh and M. Zhao (2012), "Increase of global monsoon area and precipitation under global warming: a robust signal?", *Geophysical Research Letters,* **39(6)**, DOI: https://doi.org/10.1029/2012GL051037.

[9] Menon, A. Levermann, J. Schewe, J. Lehmann and K. Frieler (2013), "Consistent increase in Indian monsoon rainfall and its variability across CMIP-5 models", *Earth Syst. Dynam.,* **4**, pp.287-300.

[10] Ministry of Natural Resources and Environment (MONRE, 2016), *Climate change and sea level rise scenarios for Vietnam*, Vietnam Publishing House of Natural Resources, Environment and Cartography.

[11] N.V. Hiep, et al. (2015), *Climate change and sea level rise scenarios for Vietnam*, National project, Funded by Vietnamese Government.

[12] J.J. Katzfey, J.L. McGregor and R. Suppiah (2014), *High-Resolution Climate Projections for Vietnam: Technical Report,* CSIRO, Australia, 266pp.

[13] N.D. Mau, N.V. Thang, M.V. Khiem (2017), "Variability of the Vietnam summer monsoon for the 21st century: Projection of PRECIS model under RCP4.5 and RCP8.5 scenarios", *Journal of Climate Change Science,* **4**, pp.25-33.

[14] National Centers for Atmospheric Research Staff (Eds) (2016), *The Climate Data Guide: Climate Forecast System Reanalysis (CFSR),* Last modified 05 Jul retrieved from https://climatedataguide.ucar.edu/climate-data/climate-forecast-system-reanalysis-cfsr.

[15] National Center for Atmospheric Research Staff (Eds) (2017), *The Climate Data Guide: APHRODITE: Asian Precipitation - Highly-Resolved Observational Data Integration Towards Evaluation of Water Resources*, Last modified 27 Feb, retrieved from https://climatedataguide.ucar.edu/climate-data/aphrodite-asian-precipitation-highly-resolved-observational-data-integration-towards.

[16] M. Hirai, T. Sakashita, H. Kitagawa, T. Tsuyuki, M. Hosaka, and M. Oh'izumi (2007), "Development and validation of a new land surface model for JMA's operational global model using the CEOP observation dataset", *J. Meteor. Soc.*, pp.1-24.

[17] K. Saito, T. Fujita, Y. Yamada, J. Ishida, Y. Kumagai, K. Aranami, S. Ohmori, R. Nagasawa, S. Kumagai, C. Muroi, T. Kato, H. Eito, and Y. Yamazaki (2006), "The operational JMA nonhydrostatic mesoscale model", *Mon. Wea. Rev.,* **134**, pp.1266-1298.

[18] A. Kitoh, T. Ose, K. Kurihara, S. Kusunoki, M. Sugi, and KAKUSHIN Team-3 Modeling Group (2009), "Projection of changes in future weather extremes using super-high-resolution global and regional atmospheric models in the KAKUSHIN Program: Results of preliminary experiments", *Hydrol. Res. Lett.,* **3**, pp.49-53.

[19] H. Sasaki, K. Kurihara, A. Murata, M. Hanafusa, and M. Oh'izumi (2013), "Future changes of snow depth in a non-hydrostatic regional climate model with bias correction", *SOLA,* **9**, pp.5-8.

[20] Kieu-Thi X., H. Vu-Thanh, T. Nguyen-Minh, D. Le, L. Nguyen-Manh, I. Takayabu, H. Sasaki, and A. Kitoh (2016), "Rainfall and tropical cyclone activity over Vietnam simulated and projected by the non-hydrostatic regional climate model", *J. Meteor. Soc. Japan,* pp.135-150, doi:10.2151/jmsj.2015-057.